RSC Advances

PAPER

View Article Online
View Journal | View Issue

Check for updates

Cite this: *RSC Adv.*, 2023, **13**, 16352

Synthesis, characterization and performance of lignin carboxyl betaine zwitterionic surfactants for application in enhanced oil recovery

Shuyan Chen,[ab] Xueliang Li,[c] Qin Lei,[a] Yuhua Han,[a] Xunping Zhou*[a] and Jianan Zhang*[d]

The objective of this study was to synthesize lignin carboxyl betaine zwitterionic surfactants (LCBS) from alkali lignin through a three-step reaction involving epoxidation, amination, and quaternization. The synthesized LCBS were characterized using infrared spectroscopy (IR) and thermogravimetric (TG) analysis. To assess their potential for enhanced oil recovery (EOR), the physicochemical properties of the LCBS surfactants, such as surface tension, emulsification, temperature resistance, salt resistance, and interfacial properties, were evaluated using standard experimental methods for surfactants applied in oil displacement. The LCBS surfactants exhibited higher surface activity, with low surface tension values ranging from 29.65 mN m^{-1} to 31.85 mN m^{-1} at the corresponding critical micelle concentration (cmc), also the significant emulsifying performance of LCBS surfactants was proved in the emulsifying experiments. Moreover, the synthesized LCBS surfactants were found to be suitable for use in harsh reservoirs of high-salinity and high-temperature, as confirmed by the temperature and salt resistance measurements. The interfacial tension (IFT) tests between Huabei crude oil and LCBS surfactants suggested that these surfactants could effectively extract the crude oil containing heavy components such as colloid and asphaltene, and ultra-low IFT values could be achieved with the addition of weak alkali.

Received 28th March 2023
Accepted 17th May 2023

DOI: 10.1039/d3ra02028b

rsc.li/rsc-advances

Open Access Article. Published on 31 May 2023. Downloaded on 2/7/2026 9:33:21 PM.
This article is licensed under a Creative Commons Attribution-NonCommercial 3.0 Unported Licence.

1. Introduction

The rapid growth of the country's economy has led to an increasing demand for energy, particularly for petroleum, which is crucial for the country's survival and development. As energy resources become increasingly scarce, enhanced oil recovery (EOR) techniques have become a key focus of petroleum exploration research.[1–3] In recent years, surfactant-centered oil displacement systems have gained more and more attention in EOR research due to their ability to significantly increase oil recovery and their relatively simple injection process.[4] Surfactant flooding primarily works by reducing the interfacial tension (IFT) of oil–water, increasing the capillary number, and extracting crude oil from rock pores to improve oil recovery.[5,6] At present, the anionic surfactants are the most commonly used oil-displacing agents in EOR, followed by non-ionic surfactants.[7] However, for high-temperature and high-salinity reservoirs, which account for a significant proportion of petroleum reserves in China, anionic surfactants exhibit good temperature tolerance but poor salt tolerance,[8] while non-ionic surfactants possess superior salt resistance but poor temperature resistance.[9] Thus, conventional surfactants cannot simultaneously provide low IFT values and wide applicability. As a result, the development of surfactants with low IFT values and high temperature and salt resistance has become a major research focus in surfactant flooding technologies.

Betaine surfactants are one of the zwitterionic surfactants used in EOR both domestically and internationally recently due to their unique inner salt structure.[10] Compared to other zwitterionic surfactants, betaine surfactants have a neutral salt structure with a wide isoelectric range and exhibit good chemical stability in acidic or alkaline media.[11] Meanwhile, the surface activity and interfacial properties of betaine surfactants are not significantly affected by the solution salinity or pH value, and they exhibit chelating effect on metal ions, effectively reducing the oil–water IFT in high-temperature and high-salinity reservoirs.[12,13] In recent years, betaine surfactants have attracted researchers' interest due to the need for the development of alkali-free and ultra-low IFT oil-displacing systems in surfactant flooding. Among them, the carboxyl betaine surfactants have garnered attention from EOR researchers and have progressed from laboratory research to field testing stages due to their unique properties, such as favorable temperature and salt resistance, excellent synergistic effects, good solubility in

[a]*Department of Environment and Quality Test, Chongqing Chemical Industry Vocational College, Chongqing 401228, China. E-mail: Zxping2021@126.com*
[b]*Chongqing (Changshou) Industrial Technology Research Institute of Green Chemical and New Material, Chongqing 401228, China*
[c]*Beijing Centre Biology Co., Ltd, Beijing 102200, China*
[d]*Institute of Nuclear and New Energy Technology, Tsinghua University, Beijing 100084, China. E-mail: zhangja@tsinghua.edu.cn*

© 2023 The Author(s). Published by the Royal Society of Chemistry

Open Access Article. Published on 31 May 2023. Downloaded on 2/7/2026 9:33:21 PM. This article is licensed under a Creative Commons Attribution-NonCommercial 3.0 Unported Licence.

various pH solutions, good surface activity, low adsorption loss, biodegradability, and more.[14,15] And the carboxyl betaine surfactants used currently for oil displacement can achieve ultra-low IFT values between brine and crude oil,[16] even after four-stage adsorption of formation sand.[17] Research has shown that betaine surfactants containing benzene ring structures in the lipophilic group can achieve ultra-low IFT values at lower concentrations than those containing aliphatic chains.[18] However, long synthetic routes, complicated technological processes, and high raw material costs have limited the widespread use of betaine surfactants in EOR. Therefore, developing highly efficient, inexpensive, and chemically stable betaine surfactants is the crucial for their implementation in EOR. The current hotspot in surfactant development for EOR involves the use of natural renewable resources to prepare environmentally-friendly and biodegradable surfactants through chemical modification.[19,20]

Lignin, a type of renewable and cost-effective natural biomass resource, is a high-molecular polymer composed of phenylpropane monomers.[21–23] The efficient conversion of lignin into high-value aromatic compounds can significantly improve the economy and sustainability of biomass resource utilization. Additionally, there are various functional groups on the benzene ring and side-chain of lignin molecular, including hydroxyl (–OH), alkyl, carbonyl (–CO–), methoxy ($–OCH_3$), and more.[24,25] Various hydrophilic or lipophilic groups can be introduced into the lignin structure through diverse chemical modification methods, improving its water solubility and surface activity.[26] Since lignin is the only natural source of aromatic groups, surfactants derived from lignin have excellent performance and are easily biodegradable. And lignin can be obtained not only from lignocellulosic renewable biomass resources such as crop stalks but also from the waste liquid produced in the pulping and paper industry.[27] As an abundant and low-priced biomass resource, lignin has great potential for application in EOR field.

Up to now, there have been numerous studies on the betaine-type amphoteric surfactants derived from lignin, but most of them have focused on the lignin sulfobetaine surfactants synthesized through sulfonation and Mannich reaction.[28] And these surfactants have been used as porous materials,[29] dispersants,[30] oil-displacing agents,[31] and promote lignocellulase.[32] Although some studies have investigated the synthesis and application of lignin carboxylates, particularly lignin carboxylates prepared through carboxymethylation modification,[33] these studies have mainly focused on the dispersion stability[34] and adsorption properties[35] of the lignin carboxylate samples. There is very little research on the synthesis and application of lignin carboxyl betaine surfactants in EOR field. In this study, we synthesized lignin carboxyl betaine surfactants (LCBS) using alkali lignin as raw materials through a three-step route of alkoxy, amination, and quaternization reaction, as shown in Scheme 1. The FT-IR was used to characterize the structure of alkali lignin and synthesized surfactants. We also experimentally investigated the physicochemical properties of LCBS surfactants, such as thermal stability, surface properties, emulsification, temperature resistance, and salt resistance, to determine their suitability for EOR applications. Moreover, we examined the interfacial behavior of LCBS surfactants to provide new ideas and a theoretical basis for the utilization of lignin in the oilfield chemicals.

2. Experimental

2.1. Material

The alkali lignin raw material was sourced from Shandong Paper Mill in Shandong, China. Aladdin Industrial Corporation in Shanghai, China provided tetrabutylammonium bromide (99.0 wt%), epichlorohydrin (99.0 wt%), sodium chloroacetate (98.0 wt%), dimethylamine (30% solution in methanol), diethylamine (99.0 wt%), and diethanolamine (99.0 wt%). Sinopharm Chemical Reagent Co., Ltd. in Beijing, China supplied sodium chloride (99.5 wt%), sulfuric acid (95.0–98.0 wt%), calcium chloride (96.0 wt%), benzene (99.5 wt%), sodium hydroxide (96.0 wt%), ethanol (95 wt%), and petroleum ether. All the chemical reagents employed in the experiments are of analytical pure grade. The crude oil used for the IFT tests was extracted from Huabei Oilfield in China, and its nature is listed in Table 1. The ionic composition of simulated brine with a total salinity of 10 789 mg L^{-1} is shown in Table 2.

2.2. Synthesis

2.2.1. Synthesis of epoxidized lignin. In step 1 of Scheme 1, 10 g of alkali lignin obtained from Shandong Paper Mill was dissolved in 100 mL of 5.0 wt% sodium hydroxide solution in a 250 mL round-bottom flask. 0.2 g of tetrabutylammonium bromide was added to the mixture, and the temperature was increased to 60 °C with stirring. Then, 6 g of epichlorohydrin was added dropwise and the mixture was refluxed at 70 °C for 6 hours. After the reaction, the excess solvent was removed under reduced pressure, and the mixture was washed with water several times through centrifugation to remove the alkali agent and any unreacted lignin. The residual epichlorohydrin was further extracted using benzene, and the product was washed with water until neutral and dried in a vacuum oven to obtain epoxidized lignin.

2.2.2. Synthesis of aminated lignin. In step 2 of Scheme 1, the epoxidized lignin was mixed with the dimethylamine solution in a molar ratio of 1.0 : 1.3 and added to a three-necked round-bottom flask. The reaction was then carried out for 6 hours at 140 °C. After the reaction, the crude product was washed with water multiple times to remove any unreacted dimethylamine, and the solid product obtained after centrifugation was aminated lignin.

2.2.3. Synthesis of lignin carboxyl betaine surfactants. In step 3 of Scheme 1, aminated lignin (25 g) and purified water (150 mL) were added to a round-bottom flask, and the pH of the solution was adjusted to 12 by adding 20 wt% sodium hydroxide solution until the aminated lignin completely dissolved. Next, 43 g of 30 wt% sodium chloroacetate solution was added dropwise over 30 minutes and refluxed at 80 °C for 9 hours. After the reaction, most of the water was removed by rotary

Open Access Article. Published on 31 May 2023. Downloaded on 2/7/2026 9:33:21 PM.
This article is licensed under a Creative Commons Attribution-NonCommercial 3.0 Unported Licence.

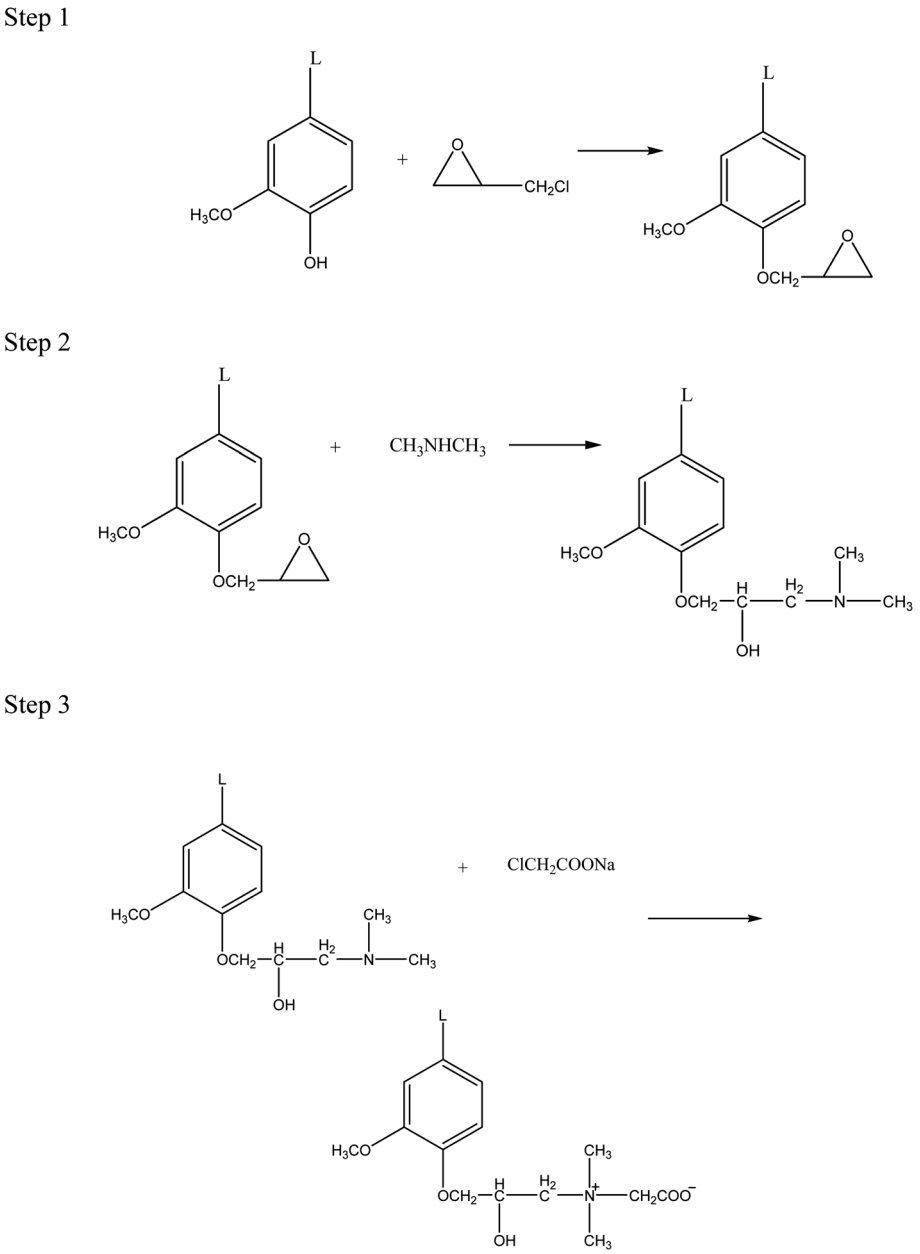

Scheme 1 Synthetic route of LCBS surfactant.

Table 1 The nature of crude oil from Huabei Oilfield, China

Oilfield	Density (20 °C) (g cm^{-3})	Condensation point (°C)	Kinematic viscosity (50 °C) (mm^2 s^{-1})	Gum content (wt%)	Wax content (wt%)	Residual carbon content (wt%)
Huabei	0.8837	36	57.10	23.2	22.8	6.7

evaporation, and the unreacted aminated lignin was extracted by washing with petroleum ether 3–4 times. And the lignin carboxyl betaine surfactants were obtained by removing the solvent. By using different organic amines (dimethylamine, diethylamine, and diethanolamine), three types of lignin carboxyl betaine surfactants were synthesized *via* this method, and the obtained products were labeled as LCBD, LCBE, and LCBT, respectively.

2.2.4. FTIR characterisation. The alkali lignin and synthesized samples were prepared using the potassium bromide (KBr) tablet method. Fourier transform infrared spectroscopy (FT-IR) was used to characterize the structure of the alkali lignin

 © 2023 The Author(s). Published by the Royal Society of Chemistry

Open Access Article. Published on 31 May 2023. Downloaded on 2/7/2026 9:33:21 PM. This article is licensed under a Creative Commons Attribution-NonCommercial 3.0 Unported Licence.

Table 2 The composition of simulated brine from Huabei Oilfield, China

Oilfield	Ca^{2+} (mg L^{-1})	Mg^{2+} (mg L^{-1})	Na^{+} (mg L^{-1})	K^{+} (mg L^{-1})	Cl^{-} (mg L^{-1})	SO_4^{2-} (mg L^{-1})	HCO_3^{-} (mg L^{-1})
Huabei	53.6	22.0	3900.7	32.2	4737.5	117.5	1925.9

and surfactants. The FT-IR analysis was conducted using a WQf-510 instrument (China) with a frequency range of 500 cm^{-1} to 4000 cm^{-1}. The number of scans used was 32, and the highest resolution was 0.85 cm^{-1}.

2.3. Measurements

2.3.1. Thermal stability measurement. The thermal properties of the LCBS surfactants were analyzed using a thermogravimetric analyzer of the SDT Q600 (TA, USA). Thermogravimetric analysis (TG) is a method that measures the weight change of a sample as it is heated, and in this study, the samples were heated from room temperature to 800 °C at a continuous heating rate of 20 °C min^{-1} under nitrogen protection with a flow rate of 50 mL min^{-1}.

2.3.2. Surface tension measurement. The surface tension of LCBS surfactants was measured using the Wilhelmy plate method at room temperature with a QBZY-2 surface tensiometer (CANY, China). Samples with mass concentration ranging from 1×10^{-6} mol L^{-1} to 1×10^{-1} mol L^{-1} were prepared and tested three times consecutively to obtain an average surface tension γ at each concentration of C. The γ–lg C curve was plotted to calculate various surface adsorption parameters, including critical surface tension (γ_{cmc}), critical micelle concentration (cmc), adsorption efficiency (pC_{20}), surface pressure at the cmc (Π_{cmc}), minimum molecular cross-sectional area (A_{min}), and saturated adsorption capacity (Γ_{max}), as per the calculation formulas described by Kamil and Siddiqui.[36] The corresponding calculation formulas are as follows:

$$pC_{20} = -\lg C_{20} \quad (1)$$

$$\Pi_{cmc} = \gamma_0 - \gamma_{cmc} \quad (2)$$

$$\Gamma_{max} = -\frac{1}{2RT}\left(\frac{d\gamma}{d \ln C}\right)_T = -\frac{1}{4.606RT}\left(\frac{d\gamma}{d \log C}\right)_T \quad (3)$$

$$A_{min} = 1/(N_A \Gamma_{max}) \quad (4)$$

where, C_{20} represents the surfactant concentration required to lower the surface tension of pure water by 20 mN m^{-1}; T is the absolute temperature (K); R is a constant of 8.314 J mol^{-1} K^{-1}; C is the concentration of surfactant (mol L^{-1}); N_A is the Avogadro constant of 6.022×10^{23} mol^{-1}.

2.3.3. Emulsification measurement. The surfactant's emulsification ability was assessed by calculating the rate of liquid drainage in the oil–water mixtures after emulsification using the stirring method. Initially, 10 mL of Huabei crude oil and 0.4 wt% of LCBS surfactants were blended at a volume ratio of 1 : 1, and the mixture was emulsified using a high-speed dispersing homogenizer at a speed of 3000 rpm for 10 minutes. The emulsion was then transferred to a colorimetric tube, and the volume of the separated liquid phase in the oil–water mixture was recorded at different time until the system was stable. The rate of water drainage was determined using the following equation:

$$q = (V_t/V) \times 100\% \quad (5)$$

where, q is the liquid drainage rate; V is the overall volume of the aqueous phase of emulsion, mL; V_t is the cumulative volume of aqueous phase at time t, mL.

2.3.4. IFT measurement. The simulated brine of Huabei Oilfield has a high salinity level of 10 789 mg L^{-1} as indicated in Table 2, in which the content of calcium and magnesium ions is relatively high. This makes Huabei Oilfield a high-salinity reservoir that requires surfactants with more stringent requirements applied in EOR. As a result, Huabei crude oil was chosen as the test oil. The IFT between LCBS solution and Huabei crude oil was measured using the XZD-SP video spinning drop interfacial tension meter (HaKe, China), with the Na_2CO_3 concentration as a variable. The test was conducted at the reservoir temperature of 54 °C of Huabei Oilfield.

2.3.5. Temperature resistance measurement. The IFT measurements were conducted using 0.4 wt% LCBS solution in simulated brine from Huabei Oilfield, and the tests were performed over a temperature range of 30 °C to 100 °C. The temperature resistance of LCBS surfactants was evaluated by measuring the variations in IFT values during the heating with temperature.

2.3.6. Salt tolerance measurement. To evaluate the salt resistance of LCBS surfactants, a series of 0.4 wt% LCBS solutions were prepared using brine with NaCl concentrations ranging from 2×10^4 mg L^{-1} to 20×10^4 mg L^{-1}. The IFT between the prepared solutions and Huabei crude oil was measured at 54 °C to examine the surfactants' resistance to univalent ions. Similarly, the salt resistance of LCBS surfactants to divalent ions was tested by measuring the IFT values in the brine containing $CaCl_2$ concentrations within the scope of 2000 mg L^{-1} to 20 000 mg L^{-1}.

3. Results and discussion

3.1. FTIR characterization

The synthesized lignin carboxyl betaine structure was exemplified using LCBD surfactant, and the FT-IR spectrum of alkali lignin (a), epoxidized lignin (b), aminated lignin (c) and lignin carboxyl betaine (d) displayed in Fig. 1 in detail. It could be seen that a broad absorption peak of O–H appeared from 3380 cm^{-1} to 3210 cm^{-1} in the alkali lignin (Fig. 1(a)), and the stretching vibration peaks of C–H band of the –CH_2– and –CH_3 groups on

Open Access Article. Published on 31 May 2023. Downloaded on 2/7/2026 9:33:21 PM.
This article is licensed under a Creative Commons Attribution-NonCommercial 3.0 Unported Licence.

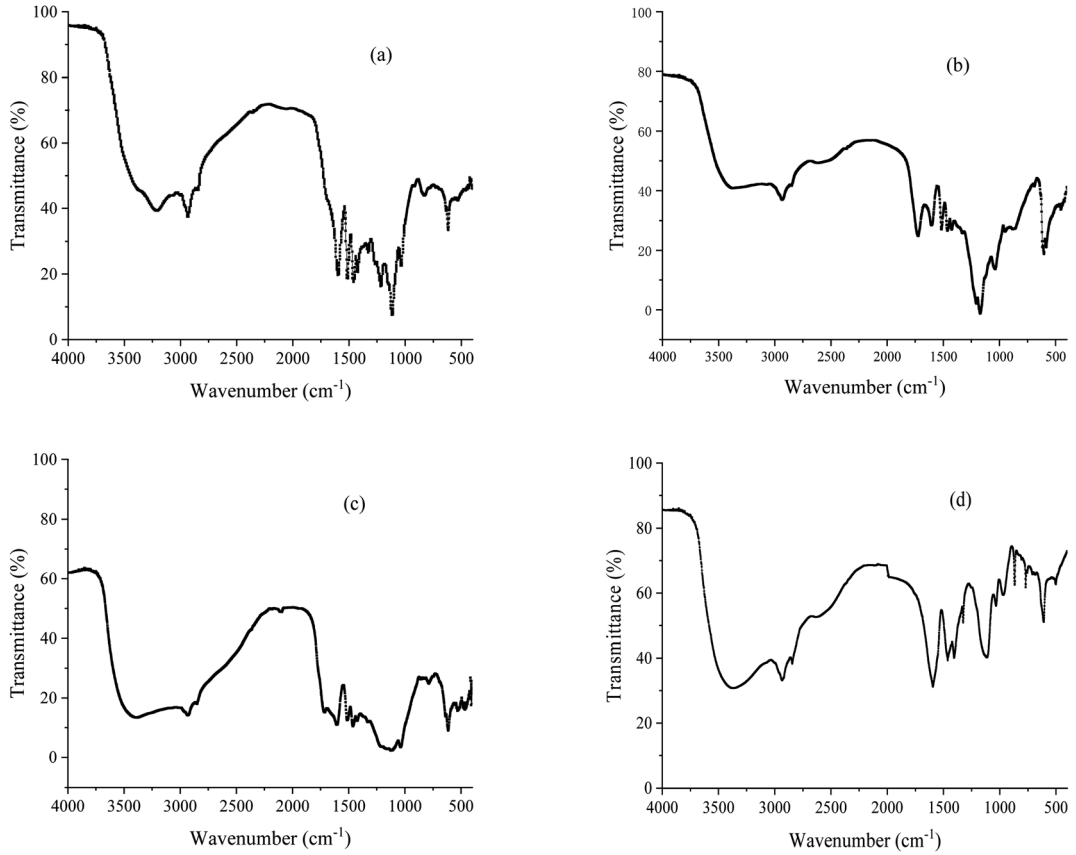

Fig. 1 FT-IR spectra of alkali lignin (a), epoxidized lignin (b), aminated lignin (c) and lignin carboxyl betaine (d).

the alkyl chain of alkali lignin could be associated with the peaks observed at 2935 cm^{-1} and 2848 cm^{-1}, respectively. The peaks observed at 1597 cm^{-1}, 1514 cm^{-1} and 1462 cm^{-1} were coupled with the characteristic peaks of the aromatic ring skeleton vibration. Compared with alkali lignin, several new absorption peaks of 910 cm^{-1} and 854 cm^{-1} appeared in the spectra of epoxidized lignin (Fig. 1(b)), which were the characteristic absorption peaks of epoxy groups. In addition, the bending vibration absorption peak of phenolic hydroxyl group at 1270 cm^{-1} in the spectrum of alkali lignin also disappeared after epoxidation, indicating that the epoxidation mainly occurred on the phenol hydroxyl group of alkali lignin. By comparing the spectrum of Fig. 1(b) and (c), it could be seen that the stretching vibration peak of C–N were clearly observed at 1320 cm^{-1} in the spectra of aminated lignin, and the disappearance of the epoxy peaks at 910 cm^{-1} and 854 cm^{-1} indicated that the epoxy group has completely reacted with the organic amine. The results indicated that the amine derivatives of alkali lignin were formed. Furthermore, the formation of the carboxyl group in the LCBD molecule was confirmed by the characteristic absorption of C=O seen at 1625 cm^{-1} (Fig. 1(d)), and the bending vibration peak and the stretching vibration peak of C–N were clearly observed at 1387 cm^{-1} and 1035 cm^{-1}, respectively, which are typically related to the characteristic absorption of quaternary ammonium salts.

3.2. Thermal stability

The prerequisite for surfactants to function as oil-displacing agents under reservoir conditions depends on their thermal stability. Surfactants are prone to decomposition at higher temperatures, especially when they migrate in the oil reservoir for a longer time. The thermal stability of three lignin carboxyl betaine surfactants (LCBD, LCBE, and LCBT) was assessed by TG analysis, and the resulting curves were depicted in Fig. 2. It

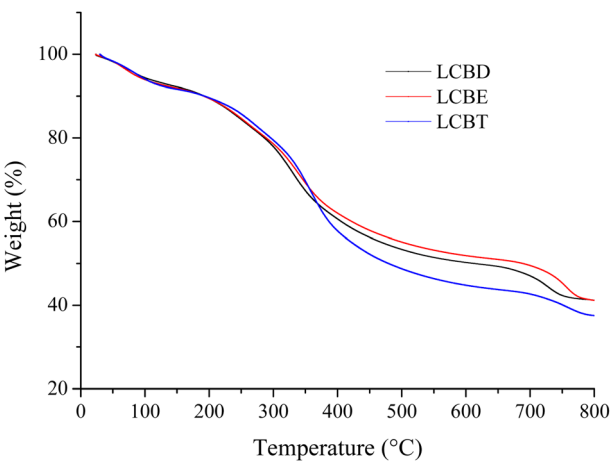

Fig. 2 TG graph of lignin carboxyl betaine.

© 2023 The Author(s). Published by the Royal Society of Chemistry

Open Access Article. Published on 31 May 2023. Downloaded on 2/7/2026 9:33:21 PM.
This article is licensed under a Creative Commons Attribution-NonCommercial 3.0 Unported Licence.

could be seen that the thermal decomposition behavior of the three surfactants was similar, and the thermal degradation process of lignin carboxyl betaine occurred in three stages with temperature. The initial weight loss percentages of LCBD, LCBE, and LCBT during the first stage (room temperature to 200 °C) were 10.51 wt%, 10.32 wt%, and 10.18 wt%, respectively, due to the loss of moisture and some impurities from the samples. The second stage (200 °C to 500 °C) was characterized by the main thermal degradation phase, which involved the surfactant decomposition. And these surfactants can be applied in most oilfields because their thermal decomposition temperatures are higher than the typical reservoir temperatures ranging from 80 °C to 120 °C.[37] During the third stage (500 °C to 800 °C), the final weight loss of LCBD, LCBE, and LCBT occurred, accompanied by the repolymerization and further depolymerization of high molecular phenolic compounds after decomposition in the previous stage until the weight loss was stable. The residue was further decomposed into carbon and ash, and the final residual mass ratio of LCBT at 800 °C was less than 40 wt%, while that of the other two surfactants was slightly higher. The higher mass loss of LCBT was due to the cleavage of more alcoholic hydroxyl groups in the LCBT molecule.

3.3. Surface tension measurement

The plot of the surface tension for lignin carboxyl betaine surfactants with concentration was presented in Fig. 3. The surface tension values sharply decreased as the surfactant concentration increased until reaching a plateau-like region, with the similar behavior observed for LCBD, LCBE, and LCBT. This can be explained by the fact that as surfactant molecules saturated the air/aqueous interface, the excess surfactant molecules will aggregate to form micelles in the aqueous solution, making further increases in the surfactant concentration have no effect on reducing the surface tension.[38] Also it can be distinctly observed that the γ–log C curve had an inflection point where the corresponding surfactant concentration and surface tension value represented the critical micelle concentration (cmc) and the γ_{cmc} at the concentration of cmc, respectively.

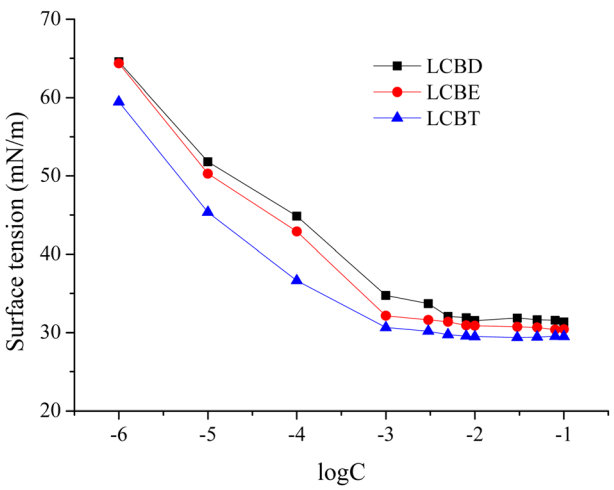

Fig. 3 Surface tension of LCBS surfactants at various concentrations.

The relevant surface adsorption parameters were calculated using formulas (1) to (4), and the value of (dγ/d log C) was obtained from the slope of the curves below the cmc in Fig. 3. Inspection data in Table 3, the γ_{cmc} of 31.85 mN m^{-1}, 31.11 mN m^{-1} and 29.65 mN m^{-1} for LCBD, LCBE and LCBT at the cmc of 4.56 mmol L^{-1}, 3.57 mmol L^{-1} and 2.29 mmol L^{-1} were acquired, respectively. Compared with LCBD and LCBE, the LCBT with a longer hydrophobic carbon chain and more hydroxyl groups exhibited lower cmc and γ_{cmc} values, suggesting that the presence of these features in the surfactant molecule affects the cmc and γ_{cmc}. This can be attributed to the fact that the surfactant's hydrophobicity increases with the growth of carbon chains, causing the surfactant molecules to arrange more closely at the air/aqueous interface, leading to the micelle formation in aqueous solutions at lower concentrations and a decrease in the cmc value.[39] Additionally, the hydrogen bond interaction generated by the hydroxyl groups in the molecule is beneficial to the surfactant molecule adsorption and aggregation, leading to the enhanced micelle formation ability and a stronger capacity of surface tension reduction in the solution.

Table 3 shows that the LCBT had a lower value of surface excess concentration (Γ_{max}) compared to LCBD and LCBE, with a larger value of area per molecule (A_{min}). This may be due to the decreased proportion of the hydrophilic head group in LCBT with increasing carbon chain length, resulting in a less tightly packed adsorption layer at the air/aqueous interface and the less overlapped of hydrophobic carbon chains.[40] Additionally, the adsorption efficiency of surfactant molecules at the air/aqueous interface can also be assessed by the pC_{20} value. A higher pC_{20} value indicates that more surfactant molecules are adsorbed at the air/aqueous interface, which is more effective to the formation of micelles and the better reduction of the surface tension of the solution. It was noted that the LCBT had a higher pC_{20} value and a lower value of surface pressure at the cmc (Π_{cmc}) compared to LCBD and LCBE, indicating that longer carbon chains in the lignin carboxyl betaine surfactant resulted in greater adsorption capacity at the gas/liquid interface. Also it could be observed that an inverse proportional relationship was observed between C_{cmc} and pC_{20} value, with smaller C_{cmc} value leading to greater pC_{20} value. In summary, surfactants with longer hydrocarbon chains and more hydroxyl groups had a greater tendency to form micelles in solution and exhibit better surface activity.

3.4. Emulsification measurement

During the surfactant flooding, the surfactant solution injected into the reservoir and the residual oil droplets exfoliated from narrow pores can form a flowable oil–water emulsion, enhancing the oil recovery ratio. In the oil–water mixture, the surfactant molecules orient themselves at the oil/water interface to form a protective film that prevents the coalescence of oil droplets, resulting in a stable oil–water emulsion. However, these emulsions are thermodynamically unstable and have a large interfacial energy, making the coalescence of emulsion

Open Access Article. Published on 31 May 2023. Downloaded on 2/7/2026 9:33:21 PM. This article is licensed under a Creative Commons Attribution-NonCommercial 3.0 Unported Licence.

Table 3 The surface adsorption parameters of LCBS surfactants

Surfactant	C_{cmc} (mmol L^{-1})	γ_{cmc} (mN m^{-1})	pC_{20}	Π_{cmc} (mN m^{-1})	Γ_{max} (mol m^{-2})	A_{min} (nm^2)
LCBD	4.56	31.85	4.78	40.15	7.41×10^{-6}	0.229
LCBE	3.57	31.11	4.92	40.89	7.25×10^{-6}	0.224
LCBT	2.29	29.65	5.52	42.35	6.54×10^{-6}	0.254

droplets a spontaneous process. As a result, the emulsion will stratify over time, and the coalescence of oil droplets will affect the displacement effect. And this experiment aimed to evaluate the emulsification efficiency of LCBS surfactants with a concentration of 0.4 wt% by investigating the drainage rate of emulsions prepared from Huabei crude oil.

Fig. 4 depicts the variation of drainage rate with time for emulsions formed using three different lignin carboxyl betaines and Huabei crude oil. The drainage rate for the emulsion prepared with LCBD initially increased rapidly with time and then stabilized at approximately 67.5 wt%. And the drainage rate for emulsions formed with LCBE and LCBT showed a similar trend with time. Additionally, it was observed that the drainage rate of emulsions decreased as the lipophilic carbon chain length of the LCBS surfactants increased, resulting in improved emulsion stability and enhanced emulsifying ability. Among the three surfactants, the emulsion prepared with LCBT reached a stable state within an hour and the drainage rate eventually stabilized at 43.6 wt%. This can be attributed to the fact that the surfactant molecules adsorb more easily at the oil/water interface as the carbon chain grows, leading to stronger intermolecular interactions and a more closely packed interfacial film arranged by the surfactant molecules. Thus, a high-strength and stable interface film with resistance to coalescence is formed, in which the coalescence speed of oil droplets is slowed down and the emulsion stability is enhanced. It means that the strength and tightness of the interfacial film play a crucial role in the formation and stability of the emulsion. Additionally, the surfactant system and crude oil exhibit good compatibility and adhesion in the relatively stable emulsion, ensuring that the crude oil can be gradually removed from the rock surface by the surfactant and cannot be easily re-adsorbed on the rock surface during the subsequent conveying process, thereby significantly improving the oil recovery efficiency.

3.5. Temperature resistance measurement

The oil–water interfacial performance is a crucial parameter during the surfactant flooding, and selecting surfactants with ultra-low IFT values ($\leq 10^{-2}$ mN m^{-1}) is the most basic requirement. However, the oil–water IFT is greatly influenced by the reservoir characteristics, particularly the temperature and salinity.[41] Hence, the temperature resistance of LCBS surfactants was firstly investigated to predict their potential application in high-temperature reservoirs. In this experiment, 0.4 wt% of LCBS solution was prepared with simulated saline and heated continuously at different temperatures ranging from 30 °C to 100 °C for 24 hours. No phenomena, such as stratification or turbidity, were observed in the solutions, and the results of IFT between LCBS solutions and Huabei crude oil at different temperatures were shown in Fig. 5. As an overall trend, the oil–water IFT values for the three lignin carboxyl betaines decreased and then increased as the temperature increased within the experimental temperature range, and the ultra-low IFT values were achieved at the temperatures ranging from 50 °C to 90 °C. These results indicate that the synthesized lignin carboxyl betaine surfactants exhibit good temperature

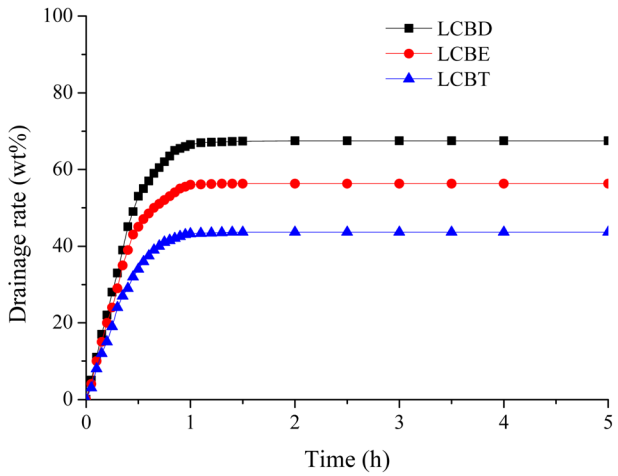

Fig. 4 The drainage rate of emulsions prepared by LCBS surfactants and Huabei crude oil as a function of time.

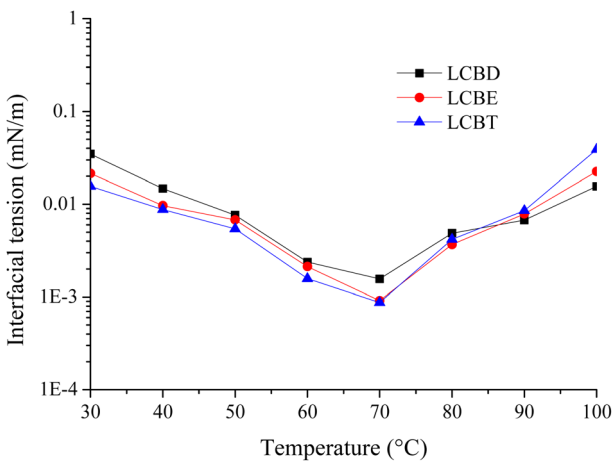

Fig. 5 Effect of temperature on IFT between LCBS surfactants and Huabei crude oil.

© 2023 The Author(s). Published by the Royal Society of Chemistry

Open Access Article. Published on 31 May 2023. Downloaded on 2/7/2026 9:33:21 PM.
This article is licensed under a Creative Commons Attribution-NonCommercial 3.0 Unported Licence.

resistance, and their interfacial activity enhances with the temperature within a certain temperature range.

As the temperature rises, the thermal motion of surfactant molecules intensifies, increasing their kinetic energy and causing a larger intermolecular distance, weakening the intermolecular attraction. This reduces the energy required for the surfactant molecule to travel from the interior of bulk solution to the surface, allowing it to escape and adsorb at the oil/water interface, ultimately reducing the value of oil–water IFT. However, continued increase in the temperature enhances the flexibility of the hydrophobic group in the surfactant molecule, leading to accelerated agglomeration and reducing the contact area with the oil phase, causing an increase in the value of oil–water IFT. It's worth noting that the IFT values for LCBT exhibited a more pronounced variation trend under high temperature compared to that of LCBD and LCBE. This is because the longer the lipophilic chain of the surfactant molecule, the more severe the agglomeration at high temperature. Although LCBT has better solubility due to its hydroxyl groups' ability to form hydrogen bonds with water molecules, these bonds are easily broken at high temperatures, compressing the diffusion electric double layer of surfactant anion and significantly reducing the hydrophilicity of surfactant. This leads to an increase in the agglomeration of the hydrophobic chains in LCBT molecules, resulting in a smaller oil–water interface layer thickness and significantly enhanced the hydrophobicity. Consequently, the oil–water IFT value increases after the precipitation of surfactant molecules from the aqueous solution due to the significantly enhanced hydrophobicity.

3.6. Salt tolerance measurement

In general, the physicochemical properties of surfactants used for injection into the formation are typically impacted by the reservoir brine in addition to the reservoir temperature. High-salinity reservoirs, in particular, can cause the surfactant precipitation, which limits their usefulness in EOR applications. To assess the salt tolerance of LCBS surfactants, we conducted an experiment to measure the IFT between Huabei crude oil and each surfactant solution containing a specific amount of NaCl (or $CaCl_2$) at 54 °C.

3.6.1. The effect of NaCl. Fig. 6 presents the IFT values between Huabei crude oil and LCBS surfactants of 0.4 wt%, which were prepared using a range of NaCl solutions with varying concentrations. The curves demonstrate that the oil–water IFT of the three LCBS surfactant solutions exhibit similar variation trends. Initially, the oil–water IFT decreased until it reached a certain concentration, where the minimum values were obtained, then increased along with the NaCl concentration. It could be seen that LCBD, LCBE, and LCBT reached their respective minimum IFT values at NaCl concentrations of 12×10^4 mg L^{-1}, 8×10^4 mg L^{-1}, and 10×10^4 mg L^{-1}, respectively. The minimum IFT value of the surfactants can only be achieved at the optimal salinity under the condition of salt addition.[42] And the optimal salinity is inversely proportional to the lipophilicity of the surfactant molecule, which means that the stronger the lipophilicity, the lower the optimal salinity. For

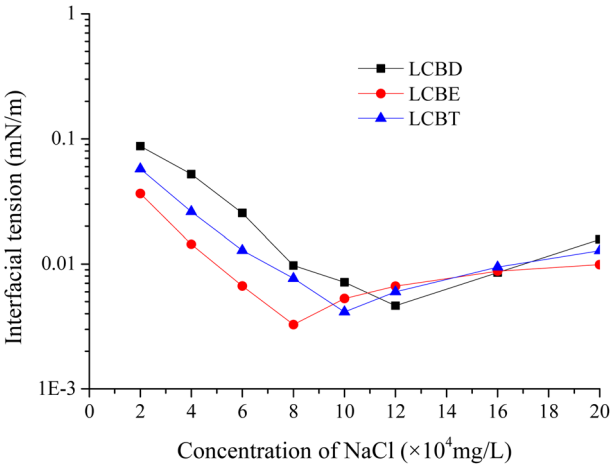

Fig. 6 Effect of NaCl concentration on the IFT between LCBS surfactants and Huabei crude oil at 54 °C.

LCBE and LCBT, although the carbon chain length in their respective surfactant molecules is similar, LCBT has a higher hydrophilicity due to its increased number of hydroxyl groups. Therefore, the minimum IFT value of LCBE can be achieved within a relatively lower salinity range. Additionally, LCBE exhibited a stronger ability to reduce the oil–water IFT compared to that of LCBD and LCBT at the same NaCl concentration, and the ultra-low IFT values of LCBE attained within the range of NaCl concentrations of 6×10^4 mg L^{-1} to 16×10^4 mg L^{-1}. Also the IFT values of the three LCBS surfactants effectively reduced the oil–water IFT to the 10^{-2} mN m^{-1} level when the NaCl concentration ranged from 8×10^4 mg L^{-1} to 16×10^4 mg L^{-1}. It could be attributed that the binding of carboxylate ions to Na^+ in solution reduces the electrostatic repulsion between the ionic head group at the oil/water interface, resulting in a more dense layer of surfactant molecules on the interface, which enabled the IFT reduction ability of LCBS surfactants to be effective over a wider salinity range. Moreover, increasing the NaCl concentration further enhanced the dissolution of LCBS surfactant in the aqueous phase, which leads to an increase in the adsorption capacity of surfactant molecules at the oil/water interface, thus reducing the oil–water IFT values. However, when the adsorption capacity of LCBS surfactant molecules at the oil–water interface reached saturation, an increase in the NaCl content will lead to the interaction between the positively charged Na^+ in the solution and the negatively charged hydrophilic groups of the surfactant increases, causing a salting-out effect that reduced the solubility of the surfactant in the aqueous phase, resulting in an increase in the oil–water IFT values.

3.6.2. The effect of $CaCl_2$. In order to gain a deeper understanding of how divalent metal ions impact the properties of surfactants at the oil–water interface, it is necessary to gather detailed information about the IFT values between Huabei crude oil and lignin carboxyl betaines with different concentrations of $CaCl_2$ at 54 °C, as depicted in Fig. 7. The curves indicated that the trend in IFT values of the three surfactants

© 2023 The Author(s). Published by the Royal Society of Chemistry

Open Access Article. Published on 31 May 2023. Downloaded on 2/7/2026 9:33:21 PM.
This article is licensed under a Creative Commons Attribution-NonCommercial 3.0 Unported Licence.

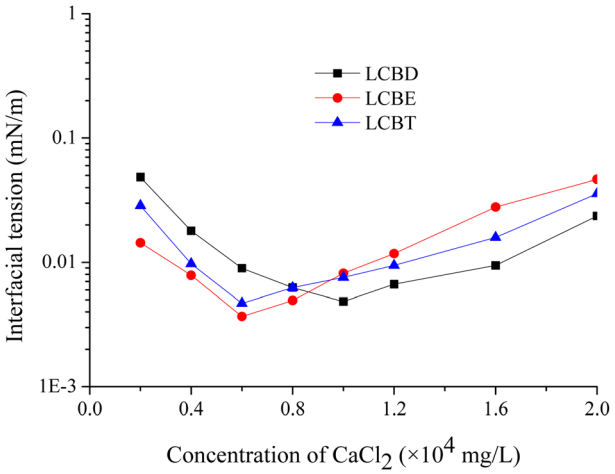

Fig. 7 Effect of $CaCl_2$ concentration on the IFT between LCBS surfactants and Huabei crude oil at 54 °C.

was similar to that of NaCl concentration (Fig. 6), the IFT reduction ability of the surfactant enhances below the optimal salinity whereas the IFT reduction ability of the surfactant reduces beyond the optimal salinity. And the optimum $CaCl_2$ concentrations of LCBD, LCBE, and LCBT were 10 000 mg L^{-1}, 6000 mg L^{-1}, and 6000 mg L^{-1}, respectively. Obviously, within the range of $CaCl_2$ concentrations from 0.6 × 10^4 mg L^{-1} to 1.2 × 10^4 mg L^{-1}, the lignin carboxyl betaine surfactants were able to achieve ultra-low oil–water IFT values, indicating their high resistance to divalent metal ions.

It should be noted that Ca^{2+} ions can cause the head groups to aggregate and the alkane chains to agglomerate due to their large charge, resulting in a stronger compression of the surfactant film than that of Na^+ ions. The addition of appropriate salts can compress the diffusion electric double layer of the hydrophilic head group, which not only shields the electrical repulsion between the ionic groups but also destroys the hydration film. This leads to a more loosely arranged surfactant film, allowing for easier penetration of oil and water molecules into the surfactant film and an increase in the thickness of the interfacial layer, ultimately resulting in a reduction in the oil–water IFT values. However, the oil–water IFT value will gradually increase if the salt concentration is further increased beyond the optimal salinity. This is because that the excessive salt ions not only shield the repulsion between polar head groups but also weaken the interaction between polar head groups and promote the agglomeration of the carbon hydrocarbon chain of the surfactant molecule, resulting in severe shrinkage of the surfactant film and a reduction in the thickness of the oil/water interface layer, therefore, the oil–water IFT value increases. It is important to note that the salinity in high-salinity reservoirs typically ranges from 10 wt% to 15 wt%,[43] and the experiments on the effects of NaCl and $CaCl_2$ on the IFT reduction of lignin carboxyl betaines suggest that these surfactants have excellent salt tolerance and can be used in both low-salinity and high-salinity reservoirs.

3.7. Oil/water interfacial tension measurement

This experiment investigated the interfacial performance of lignin carboxyl betaines and Huabei crude oil, an important indicator for selecting surfactants used in EOR. The study was conducted at Huabei reservoir's temperature of 54 °C, and the results were presented in Fig. 8. And the surfactant solutions of 0.4 wt% were used, along with Na_2CO_3 concentrations ranging from 0 to 1.2 wt%. The addition of Na_2CO_3 led to a significant reduction in the equilibrium oil–water IFT for LCBS surfactants, compared to the surfactant used alone. This reduction was observed for all three surfactants, and the IFT values continued to decrease as the Na_2CO_3 concentration increased. These findings suggest that the interfacial performance of LCBS surfactants is strongly influenced by the weak alkali of Na_2CO_3. For LCBD, the addition of 0.4 wt% Na_2CO_3 led to a two-order-of-magnitude reduction in oil–water IFT values in contrast to the LCBD alone, with similar effects observed for LCBE and LCBT. In addition, the oil–water IFT for LCBS surfactants could reach the ultra-low level as the added Na_2CO_3 concentration exceeded 0.4 wt%.

The reduction in the IFT between oil and water can be attributed to the increased adsorption of surfactant molecules on the oil/water interface, as explained by Rostami *et al.*[44] It is due to the tight arrangement of surfactant molecules on the oil/water interface, which is dependent on two factors: firstly, the polar and non-polar components of the surfactant molecules have similar affinities to the molecules present in the liquid and oil phases, respectively, and secondly, the absence of large steric hindrance among the surfactant molecules. On one hand, mixing weak alkali Na_2CO_3 in LCBS systems can result in considerable affinities of the polar and non-polar components of surfactants with the oil and liquid phases, respectively. On the other hand, Na_2CO_3 reduces the voids between the polar head groups of the surfactant molecules, resulting in a more regular permutation of surfactant molecules on the interface film and a tighter adsorption layer on the oil/water interface. Additionally, the alkali in the system can also react with the acidic components of crude oil to form surfactant-like substances, which synergistically work with the

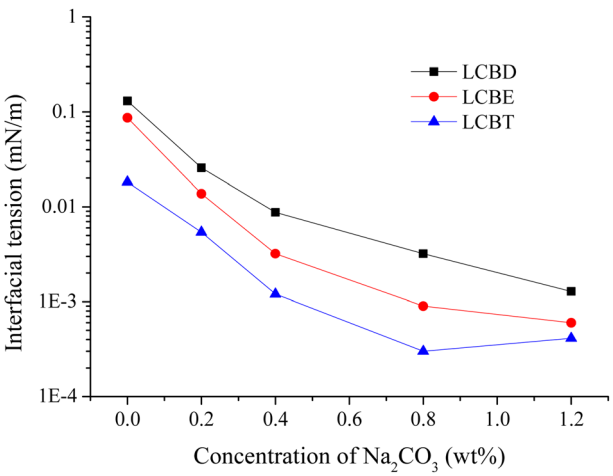

Fig. 8 Effect of Na_2CO_3 concentration on the IFT between LCBS surfactants and Huabei crude oil at 54 °C.

© 2023 The Author(s). Published by the Royal Society of Chemistry

Open Access Article. Published on 31 May 2023. Downloaded on 2/7/2026 9:33:21 PM. This article is licensed under a Creative Commons Attribution-NonCommercial 3.0 Unported Licence.

added surfactants to further lower the IFT.[45] Hence, the combined effect of LCBS and Na_2CO_3 can lower the IFT and widen the concentration range of LCBS for achieving ultra-low IFT values. Moreover, Huabei crude oil contains many asphaltene and colloidal components (as seen in Table 1), with most of the acidic components having strong interfacial activity distributed in colloid and asphaltene. Therefore, the colloids and asphaltenes present in Huabei crude oil can be adsorbed on the oil–water interface through synergistic action with lignin carboxyl betaine, helping to lower the IFT between oil and water. These results indicate that the synthesized lignin carboxyl betaines have a strong IFT reduction ability on Huabei crude oil. Additionally, Huabei reservoir's simulated brine has high salinity (as seen in Table 2), so the effect of salt on the interfacial properties of lignin carboxyl betaine must be considered. The IFT tests on Huabei crude oil, combined with the salt tolerance measurements of LCBS surfactants, confirm that the synthesized lignin carboxyl betaines are suitable for high-salinity reservoirs.

4. Conclusions

This study aimed to prepare lignin carboxyl betaine zwitterionic surfactants through a three-step process involving epoxidation, amination, and quaternization reactions from alkali lignin. The structure of the synthesized surfactants was confirmed using FTIR, and TG analysis showed that they exhibited excellent temperature stability and were resistant to decomposition below 200 °C. Also the physicochemical properties of the surfactants were evaluated to assess their applicability in the EOR field. The cmc of the LCBS surfactants was found to be between 2.29 mmol L^{-1} and 4.56 mmol L^{-1}, and their corresponding surface tension was in the range of 29.65 mN m^{-1} to 31.85 mN m^{-1}, indicating the superior surface activities. The emulsification measurements showed that the LCBS surfactants had excellent emulsifying properties, and the drainage rate of emulsions decreased with increasing hydrophobic carbon chain length. The LCBS surfactants also exhibited remarkable temperature resistance, with ultra-low IFT values achievable within the temperature range of 50 °C to 90 °C. Salt resistance measurements indicated that the LCBS surfactants could achieve ultra-low oil–water IFT values within the range of 8×10^4 mg L^{-1} to 16×10^4 mg L^{-1} of NaCl concentrations or in the range of 0.6×10^4 mg L^{-1} to 1.2×10^4 mg L^{-1} of $CaCl_2$ concentrations. The IFT tests between LCBS surfactants and Huabei crude oil revealed that the lignin carboxyl betaines exhibited better interfacial activity on the Huabei crude oil containing more heavy components such as asphaltene and colloid, and ultra-low IFT values could be achieved in the presence of weak alkali. Based on these findings, it can be concluded that the preparation of lignin carboxyl betaine surfactants from alkali lignin holds promise as an effective candidate for use in the EOR field.

Author contributions

Shuyan Chen: investigation, writing – original draft; Xueliang Li: data curation; Qin Lei: methodology; Yuhua Han: project administration; Xunping Zhou: writing – review & editing; Jianan Zhang: conceptualization, writing – review & editing.

Conflicts of interest

There are no conflicts to declare.

Acknowledgements

This work was supported by the Science and Technology Research Program of Chongqing Municipal Education Commission (Grant No. KJQN201904502; KJZD-K202004501).

References

1 A. A. Olajire, *Energy*, 2014, **77**, 963–982.
2 M. Nabipour, S. Ayatollahi and P. Keshavarz, *J. Mol. Liq.*, 2017, **230**, 579–588.
3 G. Q. Jian, Q. F. Hou and Y. Y. Zhu, *J. Dispersion Sci. Technol.*, 2015, **36**, 477–488.
4 L. F. Chen, G. C. Zhang, J. J. Ge, P. Jiang, J. Y. Tang and Y. L. Liu, *Colloids Surf., A*, 2013, **434**, 63–71.
5 F. A. Chinalia, M. B. Andrade, T. O. do Vale, S. C. dos Santos, L. F. de Moura-Costa and P. F. de Almeida, *Environ. Technol.*, 2019, **40**, 2100–2106.
6 A. Kumar and A. Mandal, *J. Mol. Liq.*, 2017, **243**, 61–71.
7 G. J. Hirasaki, C. A. Miller and M. Puerto, *SPE J.*, 2011, **16**, 889–907.
8 S. Kumar and A. Mandal, *Appl. Surf. Sci.*, 2016, **372**, 42–51.
9 J. J. Ge and Y. Wang, *J. Surfactants Deterg.*, 2015, **18**, 1043–1050.
10 H. S. M. Shakil, K. M. Shahzad and F. L. Talley, *J. Mol. Liq.*, 2018, **266**, 43–50.
11 P. Q. Li, C. Yang, Z. G. Cui, B. L. Song, J. Z. Jiang and Z. J. Wang, *J. Surfactants Deterg.*, 2016, **19**, 967–977.
12 S. M. S. Hussain, M. S. Kamal and L. T. Fogang, *J. Mol. Struct.*, 2019, **1178**, 83–88.
13 L. Y. Qi, Y. Fang, Z. Y. Wang, N. Ma, L. Y. Jiang and Y. Y. Wang, *J. Surfactants Deterg.*, 2008, **11**, 55–59.
14 Z. G. Cui, X. R. Du, X. M. Pei, J. Z. Jiang and F. Wang, *J. Surfactants Deterg.*, 2012, **15**, 685–694.
15 X. Hu, D. Qi, L. M. Yan, Z. G. Cui, B. L. Song, X. M. Pei and J. Z. Jiang, *Colloids Surf., A*, 2017, **535**, 75–82.
16 Z. G. Cui, D. Qi, B. L. Song, X. M. Pei and X. Hu, *Energy Fuels*, 2016, **30**, 2043–2051.
17 H. J. Ge, W. H. Yang and J. Cheng, *J. Chin. Cereals Oils Assoc.*, 2018, **33**, 56–59.
18 S. F. Gao, Z. Z. Song, D. Zhu, F. Lan and Q. Z. Jiang, *RSC Adv.*, 2018, **8**, 33256–33268.
19 Q. Q. Zhang, B. X. Cai, W. J. Xu, H. Z. Gang, J. F. Liu, S. Z. Yang and B. Z. Mu, *Colloids Surf., A*, 2015, **483**, 87–95.
20 P. Foley, A. Kermanshahi Pour, E. S. Beach and J. B. Zimmerman, *Chem. Soc. Rev.*, 2012, **41**, 1499–1518.
21 H. Hatakeyama and T. Hatakeyama, *Adv. Polym. Sci.*, 2010, **232**, 1–63.
22 C. Li, C. Chen, X. F. Wu, C. W. Tsang, J. H. Mou, J. B. Yan, Y. Liu and C. S. K. Lin, *Bioresour. Technol.*, 2019, **291**, 121898.

Open Access Article. Published on 31 May 2023. Downloaded on 2/7/2026 9:33:21 PM.
This article is licensed under a Creative Commons Attribution-NonCommercial 3.0 Unported Licence.

23 S. Y. Chen, S. C. Shen, X. Yan, J. Mi, G. H. Wang, J. A. Zhang and Y. J. Zhou, *J. Dispersion Sci. Technol.*, 2016, **37**, 1574–1580.
24 T. Aro and P. Fatehi, *ChemSusChem*, 2017, **10**, 1861–1877.
25 R. Vanholme, B. Demedts, K. Morreel, J. Ralph and W. Boerjan, *Plant Physiol.*, 2010, **153**, 895–905.
26 S. Y. Chen, Y. J. Zhou, H. J. Liu, J. J. Yang, Y. Y. Wei and J. A. Zhang, *Energy Fuels*, 2019, **33**, 6247–6257.
27 M. N. Satheesh Kumar, A. K. Mohanty, L. Erickson and M. Misra, *J. Biobased Mater. Bio.*, 2009, **3**, 1–24.
28 Y. J. Xu and X. D. Fu, *Fine Chem.*, 2010, **27**, 765–768, 774.
29 Q. Ai, L. Su, Q. Zhang and G. Z. Fang, *J. Beijing For. Univ.*, 2013, **35**, 102–107.
30 M. S. Zhou, R. L. Xu, W. L. Wang, Y. X. Pang and X. Q. Qiu, *Acta Polym. Sin.*, 2015, **12**, 1414–1420.
31 S. Y. Chen, H. J. Liu, H. Sun, X. Yan, G. H. Wang, Y. J. Zhou and J. A. Zhang, *J. Mol. Liq.*, 2018, **249**, 73–82.
32 C. Cai, X. J. Zhan, M. J. Zeng, H. M. Lou, Y. X. Pang, J. Yang, D. J. Yang and X. Q. Qiu, *Green Chem.*, 2017, **19**, 5479–5487.
33 B. M. Cerrutti, C. S. D. Souza, A. Castellan, R. Ruggiero and E. Frollini, *Ind. Crops Prod.*, 2012, **36**, 108–115.
34 M. K. Konduri, F. Kong and P. Fatehi, *Eur. Polym. J.*, 2015, **70**, 371–383.
35 Y. Li, R. B. Zhao, Y. X. Pang, X. Q. Qiu and D. J. Yang, *Colloids Surf., A*, 2018, **553**, 187–194.
36 M. Kamil and H. Siddiqui, *Model. Numer. Simul. Mater. Sci.*, 2013, **3**, 17–25.
37 W. L. Dowdle and W. M. Cobb, *J. Pet. Technol.*, 1975, **27**, 1326–1330.
38 I. Mukherjee, S. P. Moulik and A. K. Rakshit, *J. Colloid Interface Sci.*, 2013, **394**, 329–336.
39 X. L. Cao, X. J. He, G. Q. Zhao, X. W. Song, Q. W. Wang, Y. B. Cao and Y. Li, *Chem. J. Chin. Univ.*, 2007, **28**, 2106–2111.
40 Z. H. Asadov, S. M. Nasibova, R. A. Rahimov, G. A. Ahmadova and S. M. Huseynova, *J. Mol. Liq.*, 2017, **225**, 451–455.
41 H. Guo, Y. Q. Li, F. Y. Wang and Y. Y. Gu, *SPE Prod. Oper.*, 2017, **33**, 353–362.
42 F. Moeini, A. Hemmati-Sarapardeh, M. H. Ghazanfari, M. Masihi and S. Ayatollahi, *Fluid Phase Equilib.*, 2014, **375**, 191–200.
43 H. Zhao, P. Zhao, B. Bai, L. Xiao and X. Liu, *J. Can. Pet. Technol.*, 2006, **45**, 49–54.
44 A. Rostami, A. Hashemi, M. A. Takassi and A. Zadehnazari, *J. Mol. Liq.*, 2017, **232**, 310–318.
45 A. Samanta, K. Ojha and A. Mandal, *Energy Fuels*, 2011, **25**, 1642–1649.

© 2023 The Author(s). Published by the Royal Society of Chemistry